Deformation and toughness of polymeric systems: 7. Influence of dispersed rubbery phase

M. C. M. van der Sanden*, J. M. M. de Kok and H. E. H. Meijer†
Centre for Polymers and Composites (CPC), Eindhoven University of Technology, PO Box 513, 5600 MB Eindhoven, The Netherlands
(Received 1 October 1993)

The deformation behaviour of ethylene–propylene–diene monomer rubber-modified polycarbonate blends (PC/EPDM; where the EPDM is adhering to the PC matrix) is studied and compared with non-adhering core–shell rubber-modified polycarbonate blends (PC/CS) using slow-speed uniaxial tensile testing and notched high-speed tensile testing. As expected, only the latter testing method reveals the existence of the critical thickness of PC as a function of temperature. At a constant ligament thickness the brittle-to-tough transition temperature (T_{BT}) strongly increases upon replacing a hole (i.e. non-adhering rubber) by adhering EPDM rubbery particles. Electron beam irradiation is applied to selectively crosslink the dispersed EPDM rubbery phase and, consequently, increase its cavitation stress (which is proportional to the dynamic shear modulus). The T_{BT} proved to be highly influenced by the thus modified cavitation stress of the dispersed phase. In terms of the energy-based criterion for the prediction of the critical thickness, this can only qualitatively be explained by (i) an increased strain energy density and/or by (ii) a change in the matrix volume involved in supplying the stored elastic energy.

(Keywords: deformation; toughness; rubber cavitation stress)

INTRODUCTION

In the previous parts of this series[1–6] the ultimate toughness of amorphous glassy polymers has been discussed extensively in terms of a network density. Below a critical thickness (ID_c) of the polymeric material the maximum degree of ductility (as dictated by the network structure) can be obtained on a macroscopic scale. The local thickness of the polymeric material was controlled by the use of thin films separated by sheets of a non-adhering (ductile) polymeric spacer or via the use of a non-adhering core–shell rubber (i.e. 'holes'). However, in practice often a compatibilized system (that automatically results in a significant degree of adhesion between the rubbery particles and the matrix) is applied in order to obtain a fine dispersion of the rubbery phase (via a lowering of the interfacial tension)[7–9]. Small particles (with a size d) result in a more efficient decrease of the average distance between the particles (ID) at a dispersed phase volume fraction (Φ_r), since:

$$ID = d\left[\left(\frac{k\pi}{6\Phi_r}\right)^{1/3} - 1\right] \quad (1)$$

where k is a constant depending on the spatial rubber particle distribution (e.g. $k=2$ for a body-centred cubic lattice) and the rubber particle size distribution.

The energy-based model, introduced in part 2[1] and extended in part 4[3] of this series, describing the phenomenon of a critical thickness was derived for non-adhering rubbery particles yielding a 'holey' system. If the rubbery particles were firmly attached to the matrix, a pronounced influence was experimentally found[5]: PS filled with 60 vol% of non-adhering rubbery particles [poly(methyl methacrylate) shell] revealed a ductile deformation behaviour with a macroscopic strain-at-break of 200%, while upon replacing the non-adhering particles by 60 vol% adhering particles (polystyrene shell) a brittle fracture with a strain-at-break of $<5\%$ was found. No explanations have been sought up to now in the previous parts of this series, e.g. using the above-mentioned simple model. However, the energy available for local brittle catastrophic fracture will certainly be influenced by the presence of any interaction between the rubbery phase and the matrix. In the literature several studies have been reported on the influence of the mechanical properties of the elastomeric filler on the occurrence and/or shift of brittle-to-ductile transitions[10–17]. However, in most of these studies more than one parameter was changed at the same time resulting in ambiguous conclusions.

This study aims at providing a better understanding of the influence of the properties of the dispersed rubbery phase on the critical thickness. Polycarbonate (PC) was chosen as a model matrix, filled with non-adhering core–shell rubbers as a reference while spherical ethylene–propylene–diene monomer (EPDM) rubber particles were used. The EPDM rubber contains a low amount of maleic anhydride groups providing a certain degree of adhesion with the PC matrix. The mechanical properties of the dispersed rubbery phase can be

* Present address: Physics Department, University of California at Santa Barbara, Broida Hall, Santa Barbara, CA 93106, USA
† To whom correspondence should be addressed

0032-3861/94/14/2995–10

controlled independently by the use of electron beam (EB) irradiation after manufacturing the specimens. EB irradiation strongly induces crosslinking of the EPDM phase[18] while the PC matrix remains virtually unaffected (at least up to irradiation doses not exceeding 400 kGy). Slow-speed uniaxial tensile testing combined with tensile dilatometry and notched high-speed impact testing are used to reveal the influence of the mechanical properties of the EPDM phase on the critical thickness of PC. Finally, the influence of adhesion between the elastomer and the matrix on the value of the critical thickness will be discussed in terms of the energy-based model.

EXPERIMENTAL

Materials

The materials used were PC (General Electric Co., Lexan 141), EPDM (Exxon, Exxelor VA 1801) and a core–shell rubber (CS) with a styrene–butadiene core and a poly(methyl methacrylate) shell and a constant average particle size of 0.2 μm [Rohm and Haas Co.; Paraloid EXL 3647; d.s.c., glass transition temperature (T_g) = −78°C]. The PC was a general purpose grade: d.s.c., T_g = 150°C; g.p.c. (tetrahydrofuran, THF), number-average molar mass, M_n = 18.5 kg mol^{-1} and mass-average molar mass, M_w = 45.5 kg mol^{-1}. The EPDM rubber contains 50–60 wt% ethylene, 50–40 wt% propylene and 0.2–2 wt% maleic anhydride (substituted at the diene monomer functionality).

Sample preparation

Before blending, the PC granules were dried at a temperature of 100°C for 36 h under vacuum conditions. Blends of PC and EPDM rubber were prepared in a double-cycle extrusion process with varying compositions of 5, 10, 15 and 25 wt% EPDM on a 25 mm co-rotating twin-screw extruder (Werner and Pfleiderer ZSK 25) with a standard screw geometry and an average barrel temperature of 260°C. A master-batch of PC/EPDM 75/25 (w/w) was prepared in the first extrusion step and the desired PC/EPDM ratio was set in the second step by the addition of pure PC. Blends of PC and CS rubber were prepared using the same processing conditions with three different compositions (5, 10 and 15 wt% rubber) in a double-cycle extrusion process, where the CS rubber is added in the first step. Tensile specimens (DIN 53 455) were injection moulded at a temperature of 260°C on a Stubbe SKM 75-80 injection moulding machine. Notched high-speed tensile samples were machined from injection-moulded plates (300°C, Arburg Allrounder 220-75-250; length × width × thickness: 60 × 12 × 3 mm) and subsequently V-shaped single-edge notched in the centre of the bar according to the Izod impact protocol (ASTM D256).

Scanning electron microscopy (SEM)

SEM (Cambridge Stereo Scan 200) was used to investigate the morphology of the injection-moulded specimens. Specimens were cut at the centre of the injection-moulded tensile bars parallel to the direction of extrusion. Subsequently, the surface of the specimens was microtomed using a glass knife at liquid-nitrogen temperature. After microtoming, the sample was etched in an oxygen plasma to remove the rubbery phase and, subsequently, coated with a conducting gold layer.

Irradiation

Slow-speed tensile specimens and notched high-speed tensile specimens were irradiated with various doses (0, 25, 50, 100 and 200 kGy). EB irradiation was carried out with a 3 MeV van de Graaff accelerator at the Interfaculty Reactor Institute (Delft), in air at room temperature. In order to investigate the influence of EB irradiation on the mechanical properties of the EPDM elastomer, governed by the crosslink density, compression moulded plates of EPDM rubber (thickness 3 mm) were also irradiated with the same doses and under the same circumstances as the tensile specimens. Shielding effects due to the presence of the PC matrix in the blends are neglected. Consequently it is assumed that the EPDM rubber in the blends will possess the same mechanical properties as the neat (irradiated) EPDM rubber.

Dynamic mechanical thermal analysis

Dynamic shear moduli of the irradiated EPDM rubber plates were measured in torsion using rectangularly shaped specimens (length × width × thickness: 60 × 10 × 3 mm) in the temperature range of −90°C up to +40°C. A Rheometrics RDS II spectrometer was used at a constant frequency of 10 rad s^{-1} and a maximum strain of 0.5%.

Molar mass measurements

G.p.c. was used to determine the M_n and M_w of irradiated PC samples. G.p.c. was performed on a Waters apparatus consisting of a 510 pump, a wisp 712 injector and a differential refractometer. Three columns were used, 10^5, 10^4 and 10^3 μ-Styragel (40°C), calibrated with monodisperse polystyrene standards using THF (0.6 ml min^{-1}) as the eluent. Irradiated PC was dissolved in THF, filtered and injected on to the columns.

Mechanical testing

Before mechanical testing tensile specimens were annealed at 100°C for 24 h under vacuum conditions to remove any unwanted traces of water.

Slow-speed tensile testing was performed on a Frank tensile machine (type 81565) at a strain rate of 8×10^{-4} s^{-1} at room temperature. All measurements were carried out five times. Slow-speed tensile dilatometry as applied in this investigation, is described in part 1 of this series[5].

Notched high-speed tensile testing has been performed on a Zwick Rel SB 3122 tensile machine equipped with a climate chamber in the temperature range of −75°C up to 50°C at a cross-head speed of 1 m s^{-1} (free sample length 20 mm). The tensile toughness (G_h) is defined as the integrated area under the recorded force–displacement curve of a high-speed fractured single-edge notched (razor-blade tapped) specimen divided by the original area behind the notch tip[2].

Finally, in order to visualize the influence of spatial particle, or hole, distribution on the deformation behaviour of PC, thin PC films (thickness 7 μm) were used containing spatially randomly distributed pores with a diameter of 3 μm (14 vol%) running perpendicular to the surface of the film through the film (Cyclopore®). The Cyclopore® films were strained using a Minimat (Polymer Laboratories; distance between clamps 15 mm) mounted on an optical transmission microscope (Olympus BH2). Rectangularly shaped specimens were viewed in transmission perpendicular to the film surface at a test

speed of $5\,mm\,min^{-1}$. During loading, pictures were taken at distinct stages of the deformation using an Olympus C-35 AD-2 camera mounted on the microscope. Plastic deformation was visualized with a polarizing filter added to improve the colour contrast.

RESULTS

The critical thickness of PC (ID_c) can be calculated using the expression that was introduced in part 2 of this series[1] and verified there for physical networks and in part 3 for chemical networks[2]. It was extended in part 4[3] to include temperature and strain rate effects and, finally, was investigated in part 6[4] for two different types of physical networks:

$$ID_c = \frac{6(\gamma + k_1 \nu^{1/2})E_1}{k_2 \nu^{-1/2} \sigma_y^2} \quad (2)$$

where γ is the van der Waals surface energy, k_1 and k_2 are constants [$k_1 = 7.13 \times 10^{-15}$ J chain$^{-1/2}$ m$^{-1/2}$ and $k_2 = 2.36 \times 10^{13}$ chains$^{1/2}$ m$^{-3/2}$ (ref. 19)], E_1 is the Young's modulus, ν is the network density (entanglement and/or crosslink density) and σ_y is the yield stress. The strain rate and temperature dependence of ID_c can be predicted via the strain rate and temperature dependence of the yield stress using the well known Eyring theory of viscosity[20]:

$$\dot{\varepsilon} = A_E \exp\left[-\frac{(\Delta E^* - V^* |\sigma_y|)}{RT} \right] \quad (3)$$

where $\dot{\varepsilon}$ is the strain rate, A_E is a constant, ΔE^* is the activation energy, V^* is the activation volume, R is the gas constant and T is the absolute temperature. The temperature and strain rate dependence of E_1 is neglected in the first approximation (which might be incorrect). (The temperature dependence of E_1 can be estimated from a strict harmonic approximation of an elastic solid[21,22], resulting in roughly the same temperature dependence as found for the yield stress.) For PC all constants of equations (2) and (3) are known from the literature: $\nu = 30 \times 10^{25}$ chains m^{-3} (refs 23 and 24), $E_1 = 2300$ MPa, $\gamma = 40$ mJ m^{-2} (ref. 19), $\ln(A_E) = 8.95 \times 10^{-5}$ (ref. 25), $\Delta E^* = 335$ kJ mol^{-1} (ref. 25) and $V^* = 1.69 \times 10^3$ m^3 mol^{-1} (ref. 25). In *Figure 1* the calculated critical thickness of PC is plotted as a function of temperature and strain rate [combination of equations (2) and (3)]. Increasing the temperature or decreasing the strain rate results in an increase of the critical thickness as already discussed for the polystyrene–poly(2,6-dimethyl-1,4-phenylene ether) model system in part 4 of this series[3]. However, if adhesion prevails a considerable influence of the mechanical properties of the elastomer on ID_c is to be expected because the matrix ligaments are separated by adhering rubbery particles that can transfer stress from the surroundings to the ligament under consideration. As a result, the stored elastic energy[1] can change due to (i) a change in matrix volume supplying the energy, (ii) a contribution of elastic energy stored in the rubbery particles and (iii) a change in strain energy density within the matrix ligament as a consequence of the altered stress state. Before investigating the influence of adhesion between the elastomer and the matrix, and/or the cavitation stress of the elastomer, on the critical thickness of PC, the uniaxial tensile testing results will be discussed briefly.

Slow-speed tensile testing

Slow-speed uniaxial tensile tests were performed on pure PC and EPDM rubber-modified PC blends. In *Figure 2* some typical results are given, showing only the initial part of the curves of pure PC (100/0) and PC/EPDM 90/10. As expected, since pure PC is a tough polymer under these relatively mild testing conditions (unnotched, strain rate $8 \times 10^{-4}\,s^{-1}$) and in accordance with the other results of this test on the more dense networks (PS-PPE 20-80[1] and epoxides[2]), no ductile-to-brittle transitions (i.e. abrupt changes in the strain-to-break) can be detected. Neat PC and PC/EPDM 90/10 both reveal a ductile deformation behaviour with a strain-at-break that equals 80% (not indicated in *Figure 2*) which is again ~60% of the theoretical draw ratio (cf. refs 2, 3 and 5).

The volume change as a function of strain reveals for neat PC a deformation mechanism that, after passing the elastic region, occurs at a constant volume. This can most certainly be ascribed to the shear deformation mechanism well known to be operative in PC[13]. Adding 10 wt% EPDM rubber to PC only results in a slight deviation

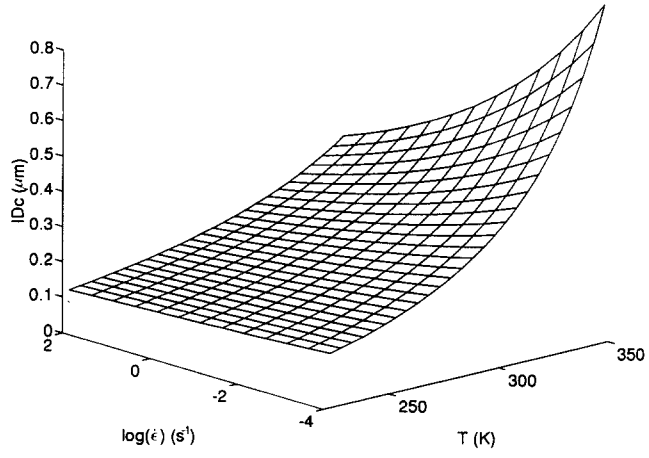

Figure 1 Model predictions of the critical ligament thickness of polycarbonate as a function of temperature and strain rate

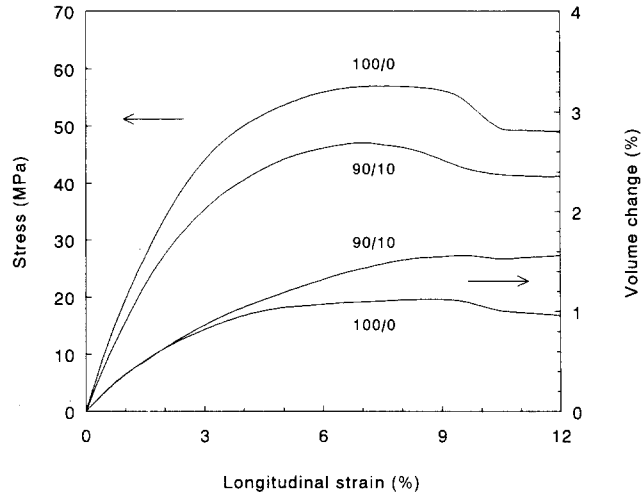

Figure 2 Initial stress–strain and volume–strain curves for PC/EPDM 100/0 and 90/10

of the $\Delta V/V_0$ curve above a strain level of 3% (*Figure 2*) probably due to the cavitation and/or detachment of the rubbery particles.

Notched, high-speed tensile testing

Unirradiated blends. The notched, high-speed tensile test results of PC/EPDM blends are displayed in *Figure 3a*. For comparison, the notched tensile toughness data of the PC/CS rubber blends are shown in *Figure 3b*. Neat PC reveals a brittle fracture over the entire temperature range investigated with a value of the notched G_h of $\sim 10\,kJ\,m^{-2}$. In contrast with the slow-speed results, brittle-to-ductile transitions can clearly be observed under notched high-speed testing conditions for both types of PC/rubber blends. As can be inferred from *Figures 3a* and *b*, the level of ductility in both the brittle and the tough region — if present — are roughly independent of the rubber concentration or type of rubber (adhering EPDM rubber or non-adhering CS rubber), while with an increasing rubber content the brittle-to-ductile transition temperature (T_{BT}) shifts to lower temperatures, from +2 to −13°C for 5 wt% to 25 wt% EPDM rubber and from −16 to −50°C for 5 wt% to 10 wt% core–shell rubber. Adding more than 10 wt% core–shell rubber does not result in a further significant lowering of the T_{BT} since

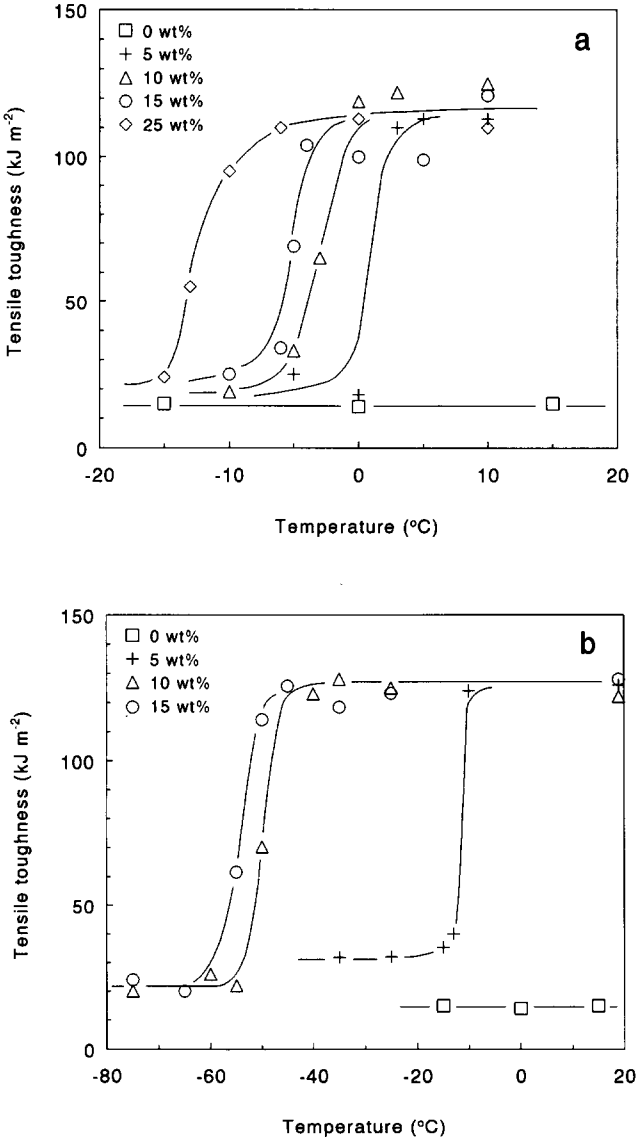

Figure 3 Notched tensile toughness (G_h) of neat and rubber-modified PC blends *versus* temperature for the rubber concentrations shown: (a) PC/EPDM; and (b) PC/CS

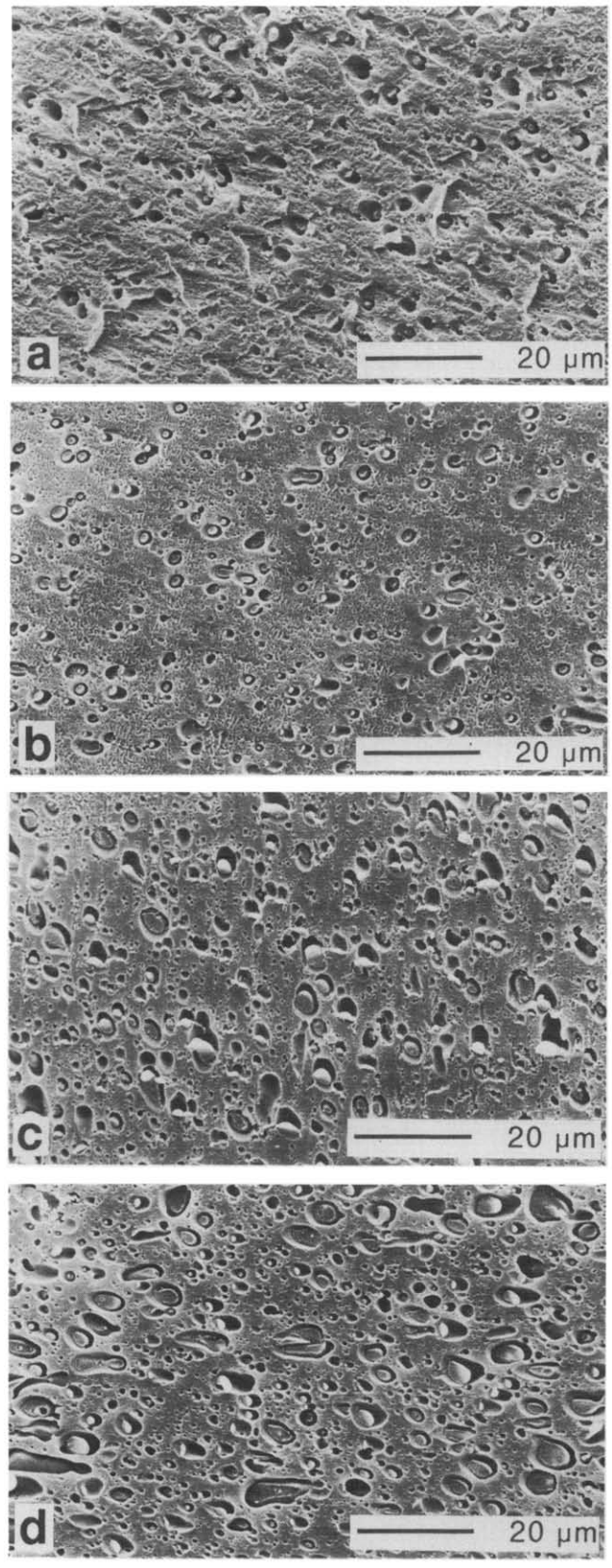

Figure 4 SEM micrographs of microtomed PC/EPDM blends: (a) 95/5; (b) 90/10; (c) 85/15; and (d) 75/25

Table 1 Weight-average particle size (d_w) and ID of the various PC/rubber blends

Blend composition (PC/rubber)	d_w (μm)	ID (μm)
PC/EPDM 95/5	0.38	0.67
PC/EPDM 90/10	0.36	0.43
PC/EPDM 85/15	0.38	0.35
PC/EPDM 75/25	0.42	0.26
PC/CS 95/5	0.2	0.35
PC/CS 90/10	0.2	0.24
PC/CS 85/15	0.2	0.18

the T_g of the core–shell rubbery particles is approached. Clearly, the holes from the core–shell rubbers are much more effective in impact modifying PC than the EPDM spheres added. This can be due to their smaller particle size (roughly two times smaller than the EPDM rubber particles, see *Figure 4* and *Table 1*) and to the absence of adhesion in the PC/core–shell rubber system.

The values of the (critical) interparticle distance that correspond to the transitions observed in *Figures 3a* and *b* can be calculated from the rubber volume fraction and the average particle size [see equation (1)]. In *Figure 4* SEM micrographs are shown of microtomed surfaces of the four different PC/EPDM blends. The average particle size is fairly constant over all compositions. This is probably due to the double-cycle extrusion process used that only dilutes the same 75/25 blend. Apparently, in this second step the average particle size hardly changes. The estimated weight-average particle sizes (d_w, obtained from SEM micrographs) of the various PC/CS and PC/EPDM blends are listed in *Table 1* combined with the corresponding values of ID, calculated using equation (1).

In *Figure 5* the T_{BT} is plotted as a function of the value of the critical thickness of PC thus determined (i.e. a cross-section of *Figures 3a* and *b*) and is compared with the predicted values according to the model (broken curve) (i.e. a cross-section at a strain rate of $10\,s^{-1}$ in *Figure 1*). Compared to the PC/EPDM blends, the PC/CS blends have a larger critical ligament thickness at a constant temperature (e.g. 0.24 *versus* 0.35 μm at -10°C) or, alternatively, shift the T_{BT} to lower temperatures at a constant value of the interparticle distance (e.g. -10 *versus* -50°C at 0.24 μm). Hence, analogous to the PS results[5], adhesion between the rubbery phase and the matrix influences the critical thickness of PC in a negative sense. Clearly, the model predictions strongly deviate from the experimentally determined values of ID_c, especially at higher temperatures (i.e. high values of ID_c). This can be ascribed to the fact that the validity of the simple model is restricted to values of ID_c comparable with or lower than the hole diameter (see Figure 7 of ref. 26). For the basic model the stored elastic energy is assumed to be correlated with a spherical volume [$\sim(ID_c)^3$]. This assumption is too naive, especially if the distance between particles is higher than the particle size used or if adhesion between matrix and dispersed phase is present.

Irradiated blends. To explore the influence of the mechanical properties of the elastomer on the brittle-to-ductile transition of PC in a controlled manner, EB irradiation of the PC/EPDM blends has been performed.

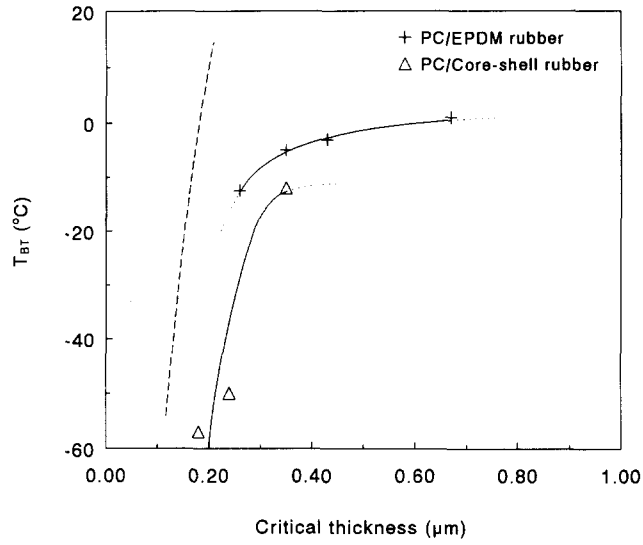

Figure 5 Brittle-to-tough transition temperature, T_{BT}, of PC/EPDM and PC/CS blends as a function of the critical ligament thickness. The broken curve is according to the model

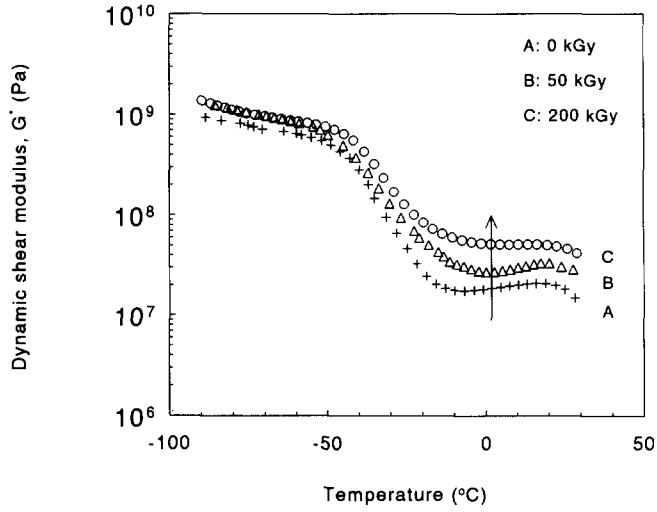

Figure 6 Dynamic shear modulus, G^*, of irradiated EPDM rubber *versus* temperature for three different irradiation doses

EB irradiation induces crosslinks in the EPDM rubber, as reflected in the dynamic shear modulus of neat EPDM rubber (*Figure 6*). EPDM rubber has a T_g of -40°C, above which a rubbery plateau is found (*Figure 6*, curve A). Irradiation of EPDM rubber results in an increase in height of this plateau. The plateau modulus (G_{No}) can be correlated with the average molecular weight between crosslinks (M_c) using classical rubber elasticity theory[27]:

$$M_c = \frac{\rho RT}{G_{No}} \tag{4}$$

Table 2 G.p.c. data of irradiated polycarbonate samples

Irradiation dose (kGy)	M_n (kg mol^{-1})	M_w (kg mol^{-1})
0	19	48
50	19	46
100	17	45
200	18	43

where ρ is the density, R is the gas constant and T is the reference temperature. Hence, an increasing value of G_{No} with increasing irradiation dose corresponds to a decreasing value of M_c. According to Gent and Tompkins[28] the Young's modulus, or shear modulus, of a rubber is directly correlated with the cavitation stress. Thus EB irradiation results in an increasing cavitation stress of the rubber, which will certainly influence the brittle-to-ductile transition of the blend provided that the adhesion remains unchanged.

The influence of EB irradiation on neat PC has been verified via g.p.c. measurements (*Table 2*) and notched high-speed tensile toughness measurements (*Figure 7a*). Clearly, within the range of irradiation doses used

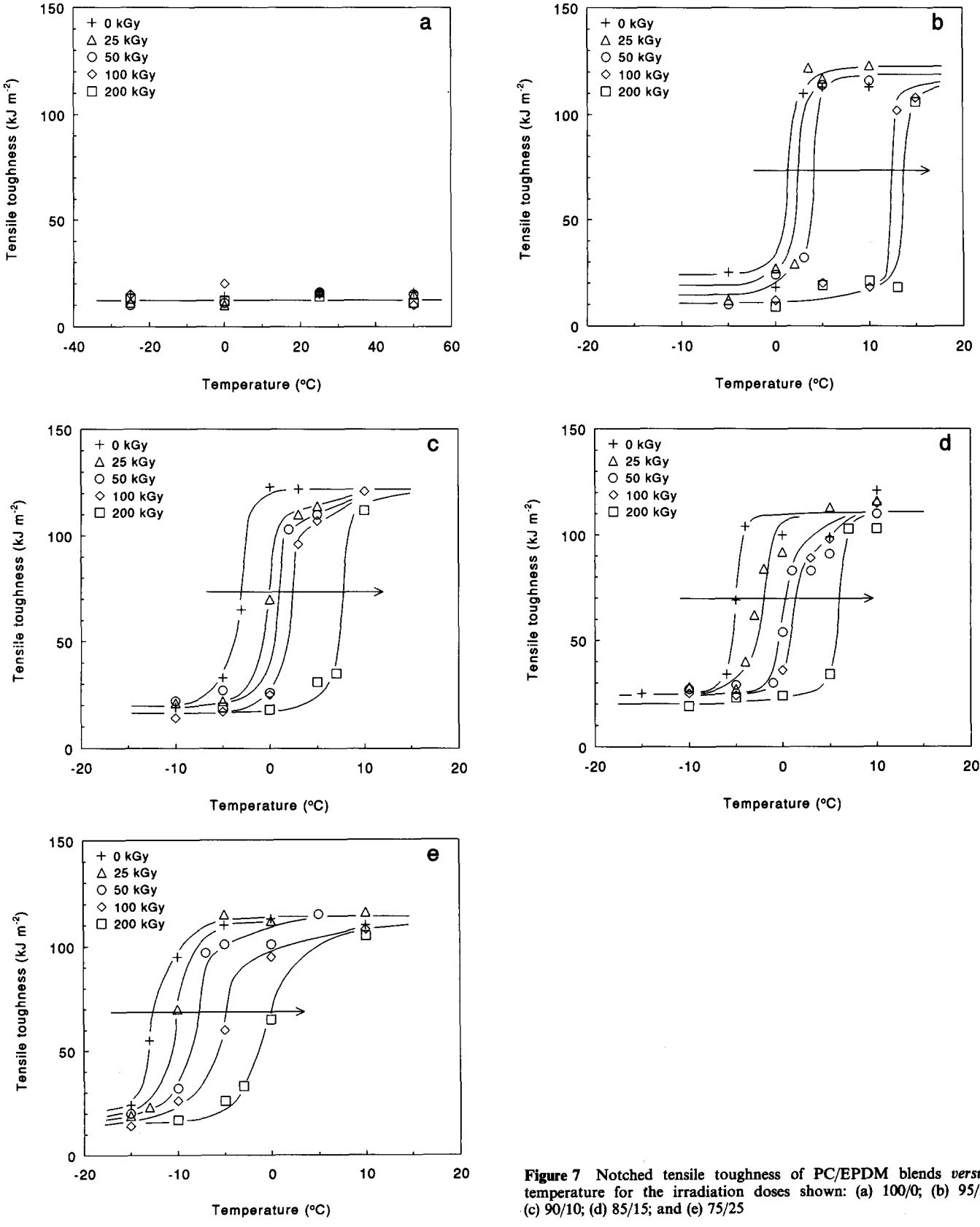

Figure 7 Notched tensile toughness of PC/EPDM blends *versus* temperature for the irradiation doses shown: (a) 100/0; (b) 95/5; (c) 90/10; (d) 85/15; and (e) 75/25

(0–200 kGy) the molecular weight of PC and the value of the notched G_h are not influenced by irradiation since the G_h value of all the PC samples is 10 kJ m^{-2}.

In *Figures 7b–e* the notched high-speed tensile toughness of the irradiated PC/EPDM blends is shown as a function of temperature for various irradiation doses. The unirradiated PC/EPDM 95/5 blend (*Figure 7b*) reveals a T_{BT} of ~2°C, while irradiation results in a shift to higher values, finally, up to +13°C for an irradiation dose of 200 kGy. The value of G_h in both the brittle and the ductile region is independent of the irradiation dose applied, similar to the independency of the value of G_h in the brittle or tough region with a varying rubber concentration (cf. *Figures 3a* and *b*).

The notched high-speed tensile data of the other PC/EPDM rubber blends all show roughly this same trend (cf. *Figures 7b–e*): irradiation results in a shift of T_{BT} to higher temperatures ($\Delta T_{BT} \approx 15$°C) independent of the absolute value of T_{BT} and the rubber concentration present in the blend. Besides, the values of G_h in both the brittle and the ductile regions remain unaffected by the irradiation dose used. To illustrate these effects, the values of T_{BT} are plotted *versus* the dynamic shear modulus, G^*, of the EPDM rubber phase in *Figure 8a*. Clearly, T_{BT} increases with an increasing G^* and the slopes of the T_{BT} *versus* G^* curves are apparently independent of the rubber concentration. At a constant G^*, T_{BT} decreases with increasing rubber concentration (i.e. a decreasing *ID*, see *Figure 8b*) similar to the conclusion arrived at during the discussion of *Figures 3a*, *3b* and *5*. *Figure 8c* contains the same data as shown in *Figure 8b* plotted on a different scale allowing for the incorporation of $T_{BT} - ID_c$ data for the PC/CS blends extracted from *Figure 5* ($G^* = 0$ MPa). According to Morbitzer and Grigo[29] the high degree of ductility of PC is related to its low γ-relaxation temperature (−100°C). Hence, it would be interesting to check this hypothesis using PC filled with real holes (foam) generating an average ligament thickness corresponding to a T_{BT} below −100°C ($\leqslant 0.1$ μm; extrapolation of *Figure 8c*).

DISCUSSION

In this series, attention has mainly focused on the understanding of the *ultimate* toughness of polymeric materials. Most conclusive evidence resulted from influencing the microstructure of amorphous polymers — given their molecular network structure — by the addition of holes using non-adhering core–shell rubber of a well-defined small size (0.2 μm). From the PS/CS systems we already know how dramatic a small change of adhesion can be[5], therefore this aspect has been chosen as the main issue here. Moreover, the PC/EPDM blends investigated are somewhat more directly related to practical blend systems that usually include adhesion between the two distinct phases. One of the reasons for this — ultimately undesired — adhesion is that small particles of a dispersed phase obviously only can be obtained during melt mixing if the two fluids are compatibilized by the addition of (block) copolymers or by their *in situ* formation[30]. For the PC/EPDM blends the resulting particle size proved to be fairly constant and of the order of 0.4 μm.

Following Borggreve[10], who investigated the toughness of the polyamide-6/EPDM system thoroughly, results of different systems can be easily compared if particle size and volume fraction are combined and converted into

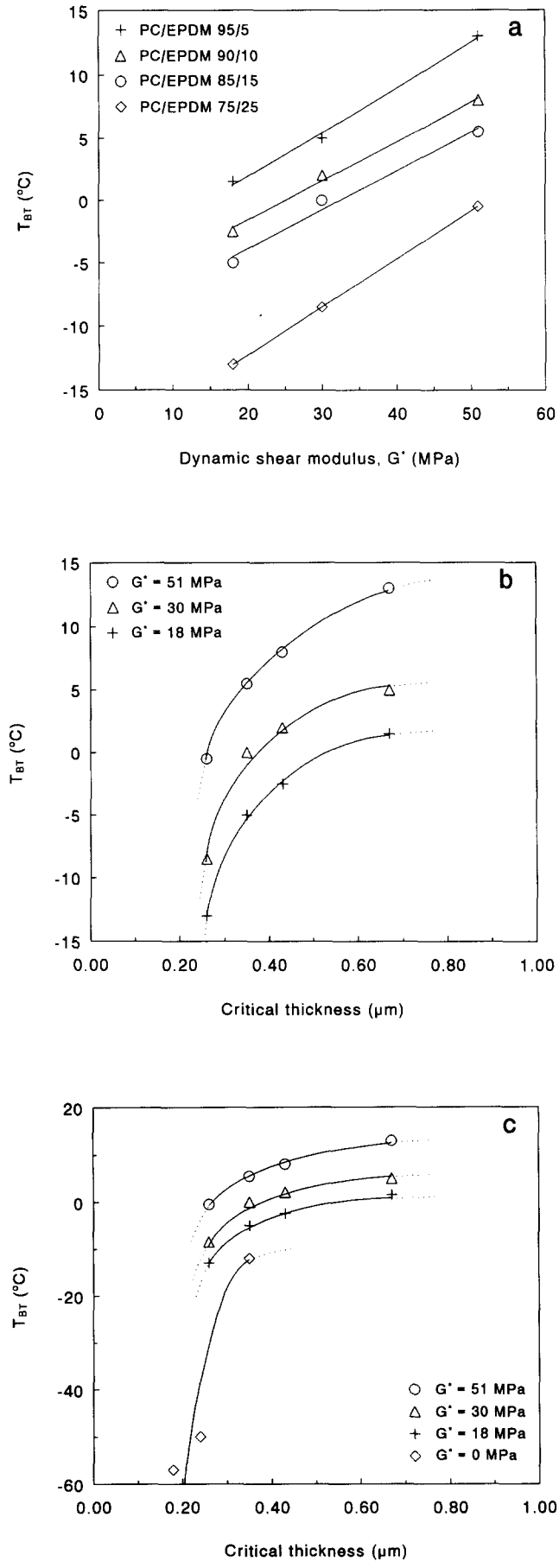

Figure 8 Brittle-to-tough transition temperature of PC/rubber blends *versus* (a) the dynamic shear modulus, G^*, of the EPDM rubber for the EPDM rubber contents shown; (b) the critical interparticle distance, ID_c, for the dynamic shear modulus values of the rubber shown; and (c) as for (b) but on a different scale

the interparticle distance, using equation (1). Comparing *Figures 3* and *5* it is clear that, after correcting for their particle size, pronounced differences between the holey, non-adhering systems (PC/CS) and adhering systems (PC/EPDM) exist, in favour of the holes. This trend is in accordance with the early PS/CS results and is subsequently confirmed by the irradiation experiments where selectively the cavitation strength of the dispersed EPDM phase is influenced without changing the morphology of the blend investigated (*Figure 8*).

The question arises whether the simple universal (but, consequently, naive) model at least qualitatively can deal with these findings. As was clearly shown, the model predictions for the critical thickness of PC are considerably lower than the experimentally determined values for the PC/CS system and did not show the pronounced temperature influence for the PC/EPDM system (*Figure 5*). Apart from these apparent defects, the introduction of adhesion and the subsequent increase of the cavitation stress systematically decreased the experimental critical thickness (*Figures 5* and *8*). It is assumed that rubber particle cavitation and/or detachment occur during or after the initiation of (localized) deformation. If cavitation and/or detachment of the particles were to occur before initiation of (localized) deformation, the stress state at the onset of plastic deformation would not be influenced by the particle cavitation and/or particle/matrix detachment stress and, consequently, the stored elastic energy would be equal to the stored elastic energy of a ligament bordered by holes and, therefore, no influence of particle/matrix detachment and/or particle cavitation stress should be observed on the value of the critical matrix ligament thickness. As mentioned, adhesion influences the volume of stored elastic energy, adds the energy stored in the dispersed phase and, finally, influences the local stress state in the matrix ligament. Since only detailed micromechanical analyses can deal with the first two aspects (which is a topic of current research in our laboratory) here only the last aspect will be discussed qualitatively focusing on the experimental trends found. Replacing a hole by an adhering rubbery particle and, subsequently, increasing the cavitation and/or detachment stress of the rubbery phase results in a more pronounced triaxial stress state in the matrix ligament. Hence the available stored elastic energy (U_{av}) will be directly influenced while the energy required to create a potential brittle fracture surface in the highly strained fibrils (U_{re}) is not changed. The strain energy density in the matrix (W_s) is given by[31]:

$$W_s=\left(\frac{1}{2E_1}\right)[\sigma_1^2+\sigma_2^2+\sigma_3^2-2\nu_m(\sigma_1\sigma_2+\sigma_1\sigma_3+\sigma_2\sigma_3)] \tag{5}$$

where σ_1, σ_2 and σ_3 are the three principal stresses and ν_m is the Poisson's ratio of the polymeric matrix ($\nu_m=0.4$ for PC). For the uniaxial stress situation where the matrix ligaments are bordered by holes it was to first order assumed that the strain energy density in the volume concerned $[(\pi/6)(ID)^3]$ is equal to the strain energy density at the equator of the hole at the matrix/hole interface:

$$W_{s,hole}=\frac{\sigma_y^2}{2E_1} \tag{6}$$

where σ_y is the uniaxial yield stress of the matrix. In the case of adhering rubbery particles (where it is assumed that cavitation and/or detachment occur after yielding of the matrix) it can be assumed that two of the three principal stresses are equal but not zero ($\sigma_2=\sigma_3=k\sigma_1$) and constant throughout the matrix volume supplying the stored elastic energy. In order to express the three principal stresses (σ_1, σ_2 and σ_3) in terms of the uniaxial yield stress (σ_y), a Von Mises yield criterion[31] is taken:

$$\sigma_y=\sqrt{\frac{(\sigma_1-\sigma_2)^2+(\sigma_3-\sigma_1)^2}{2}} \tag{7}$$

Hence, the value of W_s [equation (5)] can be expressed in the ratio $\sigma_2/\sigma_1=\sigma_3/\sigma_1=k$ (with $0\leqslant k\leqslant 1$) and normalized with the strain energy density of a matrix ligament bordered by holes, $W_{s,hole}$ ($k=0$) (*Figure 9*). Clearly, the strain energy density strongly increases with an increasing degree of triaxiality, i.e. with an increasing cavitation stress (that is proportional to the shear modulus[28]) and/or particle/matrix interface detachment stress. Consequently, a lower value of the critical ligament thickness results. Combined with the increasing matrix volume supplying stored elastic energy and the (small) contribution of the elastic energy stored in the dispersed phase, that also both result in a lower value of the critical thickness, now, qualitatively the influence of the changing properties of the adhering dispersed elastomer on the brittle-to-ductile transition can be justified. However, in order to derive a more quantitative prediction of the strain energy density and, consequently, also the critical thickness, the local stress state within the matrix ligament should be clarified more completely. This will also result in a more accurate estimation of the matrix volume that is supposed to supply the available stored elastic energy in dependence of both the level of interaction between the elastomer and the matrix and the properties of the elastomer. Eventually, these so-called multi-level finite element calculations could result in predicted values of the notched G_h in both the brittle and ductile region.

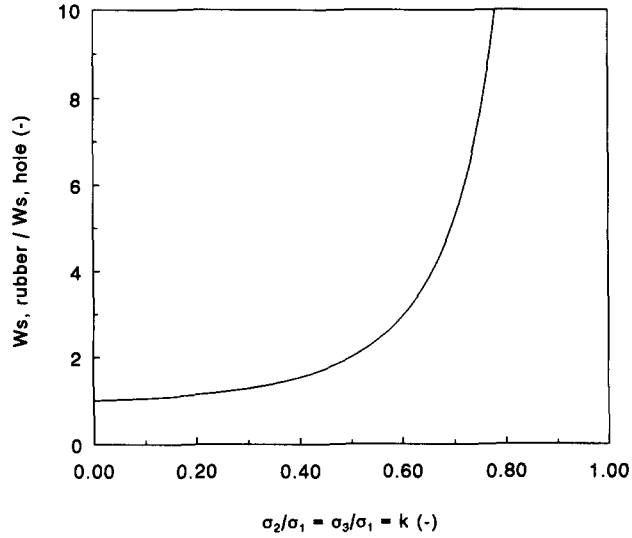

Figure 9 Normalized strain energy density of a matrix ligament bordered by adhering rubbery particles *versus* the degree of triaxiality, $\sigma_2/\sigma_1=\sigma_3/\sigma_1=k$

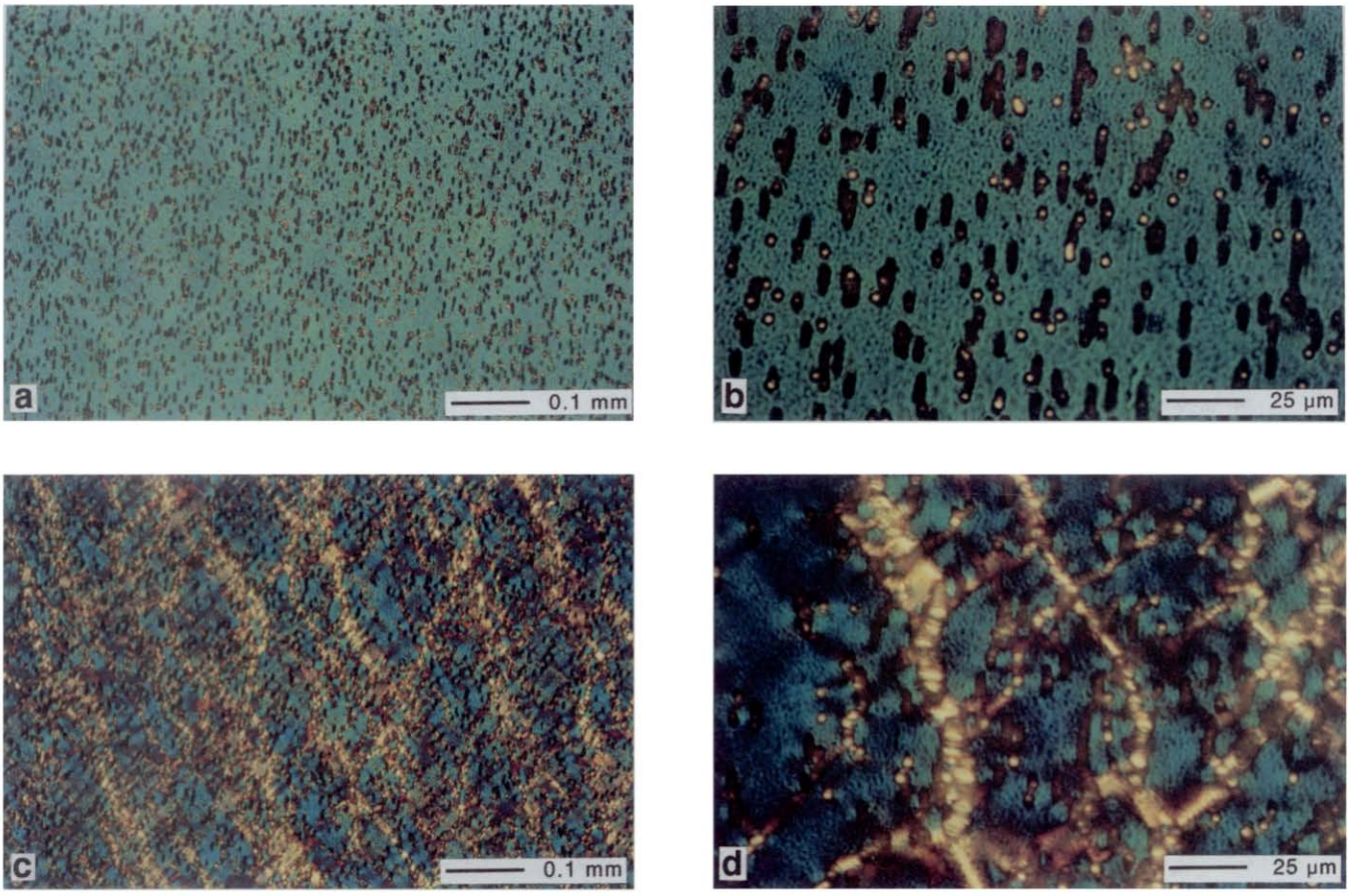

Plate 1 Polarized optical micrographs of strained porous PC films: (a) 0% strain; (b) 0% strain (high magnification); (c) 10% strain; and (d) 10% strain (high magnification)

An illustrative example

The complexity of the problems to be solved using the necessary non-uniform stress and strain fields in these calculations are illustrated in *Plate 1*, where thin PC films containing pores running perpendicular to the film surface throughout the complete film are viewed under an optical microscope during straining (direction of load: horizontal). The bright spots visible in *Plates 1a* and *b* correspond to the holes that are aligned parallel to the direction of observation. Since the pores in these films are randomly distributed, regions with a higher pore density can be easily recognized. Straining the PC film up to 10% (*Plates 1c* and *d*) results in the development of a shear band type of deformation pattern. The initiation and development of these deformation bands is clearly correlated with the inhomogeneous distribution of the pores: a higher pore density results in a higher probability of a deformation band to be initiated from this position.

CONCLUSIONS

Neat and EPDM rubber-modified PC deform via shear deformation up to 60% of the theoretical draw ratio (i.e. a strain-to-break of 80%). Notched high-speed tensile testing of rubber-modified PC as a function of temperature reveals the occurrence of a brittle-to-ductile transition with increasing temperature. At a constant ligament thickness, T_{BT} increases upon replacing holes (i.e. non-adhering core–shell rubbery particles) by adhering EPDM rubbery particles. The model predictions of the brittle-to-tough transitions of PC are much lower than the experimentally determined values, especially in the region of high ID_c values (i.e. high temperatures).

EB irradiation of the PC/EPDM blends results in a controlled crosslinking of the dispersed EPDM rubber phase while the PC matrix remains unaffected. The crosslinking of the rubbery phase results in a shift of T_{BT} to higher temperatures. A maximum shift of the T_{BT} (+15°C) is observed for the highest irradiation dose applied (200 kGy) independent of the rubber concentration present in the PC matrix (5–25 wt%). A clear correlation is established between the rubber cavitation stress (proportional to the dynamic shear modulus, G^*) and the observed T_{BT}: with increasing G^* the T_{BT} increases.

Only qualitatively, the observed dependence of the T_{BT} (or critical thickness) on the rubber cavitation and/or particle interface detachment stress can be understood in terms of an increased strain energy density in the matrix ligament as a result of an increased triaxiality of the local stress state due to the presence of adhering rubbery particles compared to the situation where the matrix ligament is bordered by holes. Moreover, the matrix volume containing the stored elastic energy is most likely to be influenced by the replacement of holes (e.g. non-adhering rubbery particles) by adhering rubbery particles. The results clearly demonstrate the necessity to comprehend the local stress state around matrix ligaments bordered by adhering elastomeric

particles which can result from (multi-level) finite element calculations.

ACKNOWLEDGEMENTS

The authors wish to thank J. M. H. Kuypens for the major part of the experimental work. A. Hiltner and E. Baer (Center for Applied Polymer Research, Case Western Reserve University, Cleveland) are acknowledged for providing the necessary facilities and L. G. C. Buijs for performing the tensile experiments under the optical microscope. The staff of the Interfaculty Reactor Institute (Delft), in particular M. Hom, are gratefully acknowledged for assistance in the irradiation experiments. This work is supported by the Foundation for Polymer Blends (SPB).

REFERENCES

1 Van der Sanden, M. C. M., Meijer, H. E. H. and Tervoort, T. A. *Polymer* 1993, **34**, 2961
2 Van der Sanden, M. C. M. and Meijer, H. E. H. *Polymer* 1993, **34**, 5063
3 Van der Sanden, M. C. M. and Meijer, H. E. H. *Polymer* 1994, **35**, 2774
4 Van der Sanden, M. C. M. and Meijer, H. E. H. *Polymer* 1994, **35**, 2991
5 Van der Sanden, M. C. M., Meijer, H. E. H. and Lemstra, P. J. *Polymer* 1993, **34**, 2148
6 Van der Sanden, M. C. M., Buijs, L. G. C., De Bie, F. O. and Meijer, H. E. H. *Polymer* 1994, **35**, 2783
7 Grace, H. P. *Chem. Eng. Commun.* 1983, **14**, 225
8 Elmendorp, J. J. *PhD Thesis* Delft University of Technology, The Netherlands, 1986
9 Elemans, P. H. M. *PhD Thesis* Eindhoven University of Technology, The Netherlands, 1989
10 Borggreve, R. J. M. *PhD Thesis* University of Twente, The Netherlands, 1988
11 Borggreve, R. J. M., Gaymans, R. J. and Schuijer, J. *Polymer* 1989, **30**, 71
12 Borggreve, R. J. M., Gaymans, R. J. and Eichenwald, H. M. *Polymer* 1989, **30**, 78
13 Parker, D. S., Sue, H-J., Huang, J. and Yee, A. F. *Polymer* 1990, **31**, 2267
14 Li, D., Li, X. and Yee, A. F. *Polym. Mater. Sci. Eng.* 1990, **63**, 296
15 Keskkula, H., Kim, H. and Paul, D. R. *Polym. Eng. Sci.* 1990, **30** (21), 1373
16 Wu, S. *Polymer* 1985, **26**, 1855
17 Yee, A. F. *J. Mater. Sci.* 1977, **12**, 757
18 Van Gisbergen, J. G. M. *PhD Thesis* Eindhoven University of Technology, The Netherlands, 1991
19 Kramer, E. J. and Berger, L. L. *Adv. Polym. Sci.* 1990, **91/92**, 1
20 Eyring, H. *J. Chem. Phys.* 1936, **4**, 283
21 Zwikker, C. 'Physical Properties of Solid Materials', Pergamon, London, 1954
22 Tabor, D. 'Gases, Liquids and Solids', Cambridge University Press, Cambridge, 1985
23 Donald, A. M. and Kramer, E. J. *J. Mater. Sci.* 1981, **16**, 2967
24 Donald, A. M. and Kramer, E. J. *J. Mater. Sci.* 1981, **16**, 2977
25 Bauwens-Crowet, C., Bauwens, J. C. and Homès, G. *J. Polym. Sci. A2* 1969, **7**, 735
26 Van der Sanden, M. C. M., Meijer, H. E. H. and Lemstra, P. J. *Progr. Colloid Polym. Sci.* 1993, **92**, 120
27 Ferry, J. D. 'Viscoelastic Properties of Polymers', Wiley, New York, 1980
28 Gent, A. N. and Tompkins, D. A. *J. Polym. Sci. A2* 1969, **7**, 1483
29 Morbitzer, L. and Grigo, U. *Angew. Makromol. Chem.* 1988, **162**, 87
30 Janssen, J. M. H. *PhD Thesis* Eindhoven University of Technology, The Netherlands, 1993
31 Williams, J. G. 'Stress Analysis of Polymers', Longman, London, 1973